ROYAL SOCIETY OPEN SCIENCE

rsos.royalsocietypublishing.org

Research

Cite this article: Nakagawa A, Aoyagi S, Omachi H, Ishino K, Nishino M, Rio J, Ewels C, Shinohara H. 2018 Isolation and structure determination of missing fullerenes $Gd@C_{74}(CF_3)_n$ through *in situ* trifluoromethylation. *R. Soc. open sci.* **5**: 181015. http://dx.doi.org/10.1098/rsos.181015

Received: 22 June 2018
Accepted: 29 August 2018

Subject Category:
Chemistry

Subject Areas:
nanotechnology/physical chemistry/synthetic chemistry

Keywords:
metallofullerenes, gadolinium, X-ray crystallography analysis, density functional calculations

Authors for correspondence:
Shinobu Aoyagi
e-mail: aoyagi@nsc.nagoya-cu.ac.jp
Haruka Omachi
e-mail: omachi@chem.nagoya-u.jp
Chris Ewels
e-mail: chris.ewels@cnrs-imn.fr

This article has been edited by the Royal Society of Chemistry, including the commissioning, peer review process and editorial aspects up to the point of acceptance.

Electronic supplementary material is available online at https://dx.doi.org/10.6084/m9.figshare.c.4224317.

THE ROYAL SOCIETY PUBLISHING

Isolation and structure determination of missing fullerenes $Gd@C_{74}(CF_3)_n$ through *in situ* trifluoromethylation

Ayano Nakagawa[1], Shinobu Aoyagi[4], Haruka Omachi[1,2], Katsuma Ishino[1], Makiko Nishino[1], Jeremy Rio[5], Chris Ewels[5] and Hisanori Shinohara[1,3]

[1]Department of Chemistry, Graduate School of Science, [2]Research Center for Materials Science, and [3]Institute for Advanced Research, Nagoya University, Nagoya 464-8602, Japan
[4]Department of Information and Basic Science, Nagoya City University, Nagoya 467-8501, Japan
[5]Institut des Materiaux Jean Rouxel (IMN), Université de Nantes, CNRS UMR6502, 2 Rue de la Houssiniere, BP32229, Nantes 44322, France

SA, 0000-0002-7393-343X; HO, 0000-0001-8513-2982; CE, 0000-0001-5530-9601

Our trifluoromethyl functionalization method enables the dissolution and isolation of missing metallofullerenes of $Gd@C_{74}(CF_3)_n$. After multi-stage high-performance liquid chromatography purification, $Gd@C_{74}(CF_3)_3$ and two regioisomers of $Gd@C_{74}(CF_3)$ are isolated. X-ray crystallographic analysis reveals that all of the isolated metallofullerenes react with CF_3 groups on pentagons of the D_{3h}-symmetry C_{74} cages. Highest occupied molecular orbital-lowest unoccupied molecular orbital gaps of these trifluoromethylated derivatives, estimated by absorption spectra, are in the range 0.71–1.06 eV, consistent with density functional calculations.

1. Introduction

Endohedral metallofullerenes $M@C_{2n}$ (M = rare earth metal), encapsulating metal atoms in the internal space of spherical carbon structures, have attracted much attention due to their unique properties [1,2]. Of these, gadolinium-encapsulated metallofullerenes have been widely investigated for biomedical applications [3–8]. With such high magnetic moments, $Gd@C_{2n}$ are of interest as novel magnetic resonance imaging (MRI) contrast agents [3–6]. The fully enclosing carbon cage completely prevents

leaching of the Gd atoms, resulting in lower toxicity than commercially available metal chelate reagents such as Gd-DTPA. However, only $M@C_{82}$ type metallofullerenes have been used for these applications. Although a lot of small-cage endohedral metallofullerenes $M@C_{2m}$ ($2m = 60$, 70, 72 and 74) are obtained in as-synthesized carbon soot, there are few examples of successful isolation [9–15]. These metallofullerenes, so-called missing (or small highest occupied molecular orbital (HOMO)–lowest unoccupied molecular orbital (LUMO) gap) metallofullerenes, are highly reactive and tend to form insoluble polymerized solids in raw soot.

Recently, we developed an *in situ* trifluoromethylation method for the extraction and purification of these missing metallofullerenes [16–19]. CF_3 groups [20–23], furnished by the thermal pyrolysis of polytetrafluoroethylene (PTFE), were introduced to the outer cages of fullerenes and stabilized reactive missing metallofullerenes during the production simultaneously. A series of yttrium- and lanthanum-encapsulated missing metallofullerenes were isolated by this technique. However structural determination still remains an important open question for fullerene science. We herein report the isolation of CF_3-functionalized $Gd@C_{74}$ and structural determination by single-crystal X-ray diffraction.

2. Method

2.1. Synthesis and purification of $Gd@C_{74}(CF_3)$ (I), $Gd@C_{74}(CF_3)$ (II) and $Gd@C_{74}(CF_3)_3$

Trifluoromethylated Gd-metallofullerenes were synthesized by the modified arc-discharge method. A cross-sectional view of the DC arc-discharge chamber is illustrated in electronic supplementary material, figure S1, where PTFE rods (40 g) are placed near the discharge area. A graphite rod (100 g) impregnated with Gd (La) (0.8 mol%, Toyo Tanso Co. Ltd) was used as the anode. A pure graphite rod (Toyo Tanso Co. Ltd) was used as the cathode. Arc discharge was performed at a DC current of 500 A in a flowing He atmosphere with a pressure of 7–9 kPa. During arc discharge, because of the high temperature around the arc zone, PTFE was decomposed and evaporated to produce CF_3 radicals. Normally, 50–70 g of raw soot was obtained per discharge. Gd-metallofullerenes and empty fullerenes were extracted from the raw soot with *o*-xylene.

2.2. Separation of trifluoromethylated Gd-metallofullerenes from empty fullerenes by $TiCl_4$

To a 500 ml CS_2 solution of the crude mixture, *ca* 5 ml of $TiCl_4$ was added. Metallofullerenes were reacted immediately and insoluble complexes were precipitated out [24–26]. After mixing for 5 min, the precipitate was collected on PTFE membrane filter and washed with 10–20 ml of CS_2 to separate from the fullerenes in solution. Deionized water was passed through the filter to decompose the complexes of metallofullerene/$TiCl_4$, and then washed with acetone to eliminate extra water. Finally, CS_2 was passed through the filter to collect the desired metallofullerenes as a solution.

2.3. Multi-stage high-performance liquid chromatography purification of Gd-metallofullerenes

High-performance liquid chromatography (HPLC) purification was conducted using a JAI (Japan Analytical Industry Co.) recycling preparative HPLC LC-9104HS. Three isomers of $Gd@C_{74}(CF_3)_n$ were isolated from the mixture by the multi-stage HPLC method. Two kinds of columns were used alternatively with toluene eluent for the isolation, i.e. Buckyprep column (20 mm diameter × 250 mm, Nacalai Tesque Inc.) and Buckyprep-M column (20 mm diameter × 250 mm, Nacalai Tesque Inc.). The initial (first-stage) HPLC purification was performed with Buckyprep-M. $Gd@C_{74}(CF_3)_3$ was obtained in fraction A and $Gd@C_{74}(CF_3)$ (I) and (II) were obtained in fraction B. The overall separation scheme and the HPLC chromatograms are shown in electronic supplementary material, figures S2–S10.

2.4. X-ray crystal structure analysis

Single crystals of $Gd@C_{74}(CF_3)$ (I) and (II) and $Gd@C_{74}(CF_3)_3$ were obtained by co-crystallization with Ni(OEP) (OEP = octaethylporphyrin) from solution. The single-crystal X-ray diffraction data were collected at SPring-8 BL02B1 [27]. The crystal structures were determined using SIR [28] and SHELX [29]. The crystallographic data are summarized in electronic supplementary material, table S1, and crystallographic information files (CIF). A theoretical D_{3h}-symmetry C_{74} rigid-body molecule was used in modelling of the $Gd@C_{74}(CF_3)_n$ molecules showing severe orientation disorder. Although the

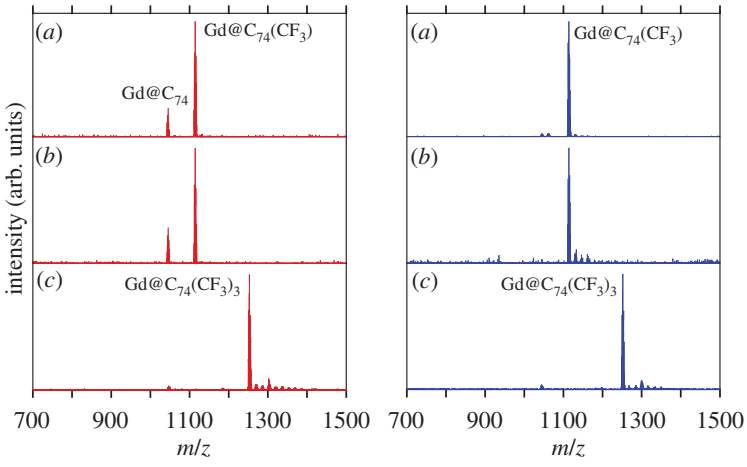

Figure 1. Mass spectra (positive-ion mode in red, negative-ion mode in blue) of (*a*) $Gd@C_{74}(CF_3)$ (I), (*b*) $Gd@C_{74}(CF_3)$ (II) and (*c*) $Gd@C_{74}(CF_3)_3$.

$Gd@C_{74}(CF_3)_n$ molecules have chiral structures, the space groups of the crystals are centrosymmetric. Therefore, each crystal contains the same number of the chiral isomers. The anisotropic atomic displacement parameters of carbon atoms on disordered C_{74} cages of $Gd@C_{74}(CF_3)$ (I) and (II) were determined by using two parameters of translation and libration motions of the rigid-body molecules [30,31]. The CIF deposition numbers at the Cambridge Crystallographic Data Centre (CCDC) are 1824999 for $Gd@C_{74}(CF_3)$ (I), 1825000 for $Gd@C_{74}(CF_3)$ (II) and 1825001 for $Gd@C_{74}(CF_3)_3$.

2.5. Density functional calculations

Density functional (DFT) calculations were performed under the local spin density approximation, as implemented in the AIMPRO code [32–34]. Relativistic pseudopotentials were included via the Hartwigsen–Goedecker–Hütter scheme [35]. For C/Gd/F, a basis set containing 38/90/28 independent Gaussian-based functions was used [36]. Calculations were fully spin polarized with spin relaxation. Periodic boundary conditions at the gamma point were used, with cell size large enough to avoid interaction between neighbouring fullerenes. A system-dependent plane wave energy cutoff of 300 Ha (Ha: Hartree energy) was applied with a non-zero electron temperature of $kT = 0.04$ eV for electronic level occupation. Atomic positions were geometrically optimized until the maximum atomic position change in a given iteration dropped below 10^{-6} a_0 (a_0: Bohr radius). The method has been previously successfully applied to study Gd-metallofullerenes [19] and is discussed in more detail in another article [37].

3. Results

The purity of the three metallofullerenes obtained by multi-stage HPLC preparation was confirmed by matrix-assisted laser desorption/ionization time-of-flight (MALDI-TOF) mass spectroscopy (figure 1). The mass spectra of the isolated samples show strong isolated peaks of $Gd@C_{74}(CF_3)$ (I and II) and $Gd@C_{74}(CF_3)_3$, respectively, confirming that these species are highly purified through the multi-stage HPLC separation. Figure 1*a–c* indicates a peak corresponding to the presence of $Gd@C_{74}$, attributed to the parent fullerene dissociated by laser-induced fragmentation. Close inspection reveals that this peak is enhanced in the positive-ion mass spectra. The preferential detection of $Gd@C_{74}$ in the positive-ion spectra results from the elimination of the electron-withdrawing CF_3 group. After the dissociation of the CF_3 moieties, the remaining $Gd@C_{74}$ tends to lose electrons and be detected as a cation [16–19]. Figure 2*a* shows the molecular arrangement of the monoclinic crystal consisting of $Gd@C_{74}(CF_3)$ (I) and Ni(OEP) in a ratio of 1 : 1. The crystal also contains toluene and chloroform solvent molecules. The disordered $Gd@C_{74}(CF_3)$ (I) molecule on the crystallographic mirror plane was modelled by a Gd atom occupying four (two independent) positions and a $C_{74}(CF_3)$ (I) molecule with six (three independent) orientations (electronic supplementary material, figure S11). The complicated disorder can be represented by an overlap of $Gd@C_{74}(CF_3)$ (I) molecules with an ordered structure shown in figure 2*d* with different orientations.

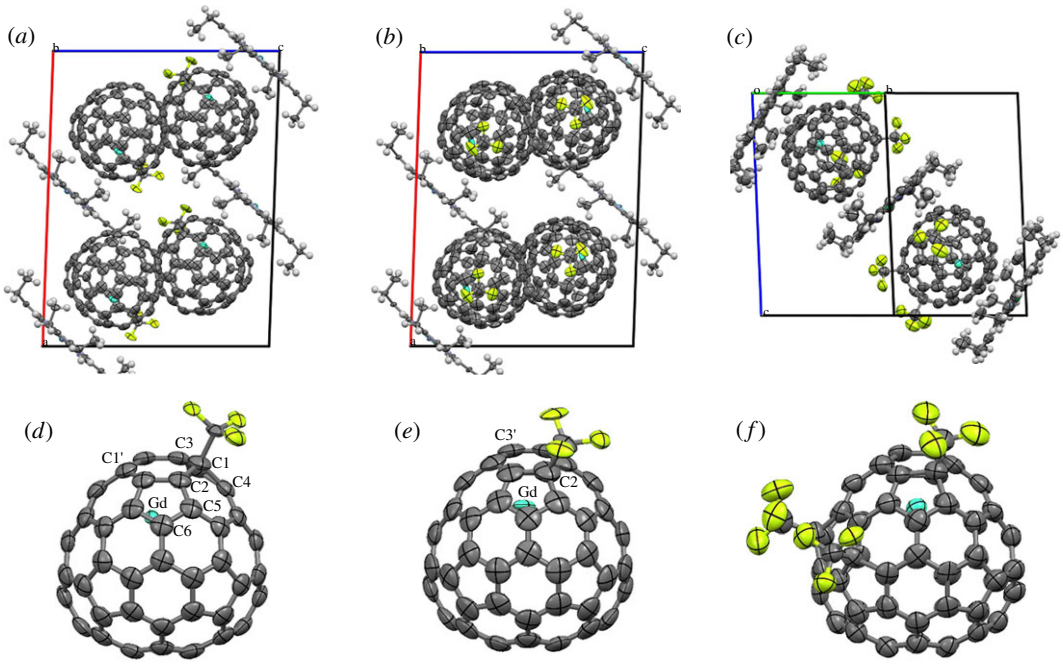

Figure 2. (*a*–*c*) Crystal structures of (*a*) Gd@$C_{74}(CF_3)$ (I), (*b*) Gd@$C_{74}(CF_3)$ (II) and (*c*) Gd@$C_{74}(CF_3)_3$, co-crystallized with Ni(OEP). The thermal ellipsoids are drawn at 50% probability level. Hydrogen atoms are drawn as small spheres. Disordered structure and solvent molecules are omitted. View along (*a*,*b*) $[1\bar{1}\ 0]$ or (*c*) $[1\bar{1}\ 0]$. (*d*–*f*) Feasible molecular structures of (*d*) Gd@$C_{74}(CF_3)$ (I), (*e*) Gd@$C_{74}(CF_3)$ (II), and (*f*) Gd@$C_{74}(CF_3)_3$ viewed along the three-fold axis of the D_{3h}-symmetry C_{74} cages.

Figure 2*d* shows a feasible molecular structure of Gd@$C_{74}(CF_3)$ (I) derived from the X-ray crystal structure analysis. A CF_3 group is attached to a carbon atom on a pentagon of the D_{3h}-symmetry C_{74} cage. The D_{3h}-symmetry C_{74} cage has six independent carbon atoms on pentagons, which are labelled as C1–C6 in the figure. The structural model with a CF_3 group attached to the C1 atom gave the best reliable factor in the X-ray crystal structure analysis of Gd@$C_{74}(CF_3)$ (I). The Gd atom locates near the carbon atom labelled as C1′ in figure 2*b*. The C1′ atom is the third nearest to the C1 atom with the CF_3 group attached. Interestingly, the C1 and C1′ atoms are equivalent in the D_{3h}-symmetry C_{74} cage with the mirror symmetry. The metal atoms of Gd@$C_{60}(CF_3)_5$ (I) and (II), La@$C_{60}(CF_3)_5$ (I) and La@$C_{70}(CF_3)_3$ also locate near a carbon atom which is the third nearest to a carbon atom with a CF_3 group attached [17,19]. The interatomic distance between the Gd and C1′ is 2.20 Å in Gd@$C_{74}(CF_3)$ (I), which is slightly shorter than Gd–C distances of 2.35 and 2.38 Å in Gd@$C_{60}(CF_3)_5$ (I) and (II), respectively [19]. On the other hand, it is slightly longer than a Gd–C distance of 2.08 Å in Gd@$C_{2v}(9)$-C_{82} [38].

The molecular arrangement and lattice constants of the Gd@$C_{74}(CF_3)$ (II) crystal are similar to those of the Gd@$C_{74}(CF_3)$ (I) crystal (figure 2*b*). Solvent molecules in the Gd@$C_{74}(CF_3)$ (II) crystal are toluene and carbon disulfide, which are different from those (toluene and chloroform) in the Gd@$C_{74}(CF_3)$ (I) crystal. The disordered Gd@$C_{74}(CF_3)$ (II) molecule on the crystallographic mirror plane was modelled by a Gd atom occupying seven (four independent) positions and a $C_{74}(CF_3)$ (II) molecule with four (two independent) orientations (electronic supplementary material, figure S12). Figure 2*e* shows a feasible molecular structure of Gd@$C_{74}(CF_3)$ (II) derived from the X-ray crystal structure analysis. The structure model with a CF_3 group attached to the C2 atom gave the best reliable factor in the X-ray crystal structure analysis of Gd@$C_{74}(CF_3)$ (II). The Gd atom in Gd@$C_{74}(CF_3)$ (II) also locates near a carbon atom (C3′) which is the third nearest to a carbon atom (C2) with the CF_3 group attached. The Gd–C3′ distance is 2.27 Å in Gd@$C_{74}(CF_3)$ (II), which is slightly longer than the Gd–C1′ distance of 2.20 Å in Gd@$C_{74}(CF_3)$ (I).

The molecular arrangement of the Gd@$C_{74}(CF_3)_3$ crystal is rather different from that of the Gd@$C_{74}(CF_3)$ (I) and (II) crystals (figure 2*c*). The triclinic crystal consists of Gd@$C_{74}(CF_3)_3$ and Ni(OEP) in a ratio of 2:3 without any solvent molecules. The disordered Gd@$C_{74}(CF_3)_3$ molecule was modelled by a Gd atom occupying three independent positions and a $C_{74}(CF_3)_3$ molecule with two independent orientations (electronic supplementary material, figure S13). Site occupancies for the major Gd position and the major $C_{74}(CF_3)_3$ orientation are 0.63 and 0.74, respectively. Figure 2*f* shows a feasible molecular structure of Gd@$C_{74}(CF_3)_3$ consisting of the Gd atom at the major position and

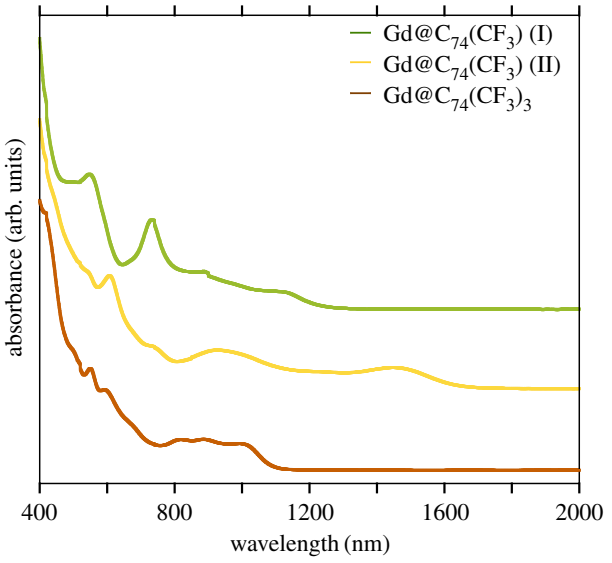

Figure 3. Absorption spectra of $Gd@C_{74}(CF_3)$ (I), $Gd@C_{74}(CF_3)$ (II), and $Gd@C_{74}(CF_3)_3$.

the $C_{74}(CF_3)_3$ with the major orientation. Three CF_3 groups of $Gd@C_{74}(CF_3)_3$ are attached to carbon atoms on three pentagons of the D_{3h}-symmetry C_{74} cage. One of the three carbon atoms with CF_3 groups attached (C2) is the same as the carbon atom with the CF_3 group attached in $Gd@C_{74}(CF_3)$ (II) shown in figure 2*e*. The Gd position in $Gd@C_{74}(CF_3)_3$ is also similar to that in $Gd@C_{74}(CF_3)$ (II). The Gd−C3′ distance is 2.34 Å in $Gd@C_{74}(CF_3)_3$, which is slightly longer than that of 2.27 Å in $Gd@C_{74}(CF_3)$ (II).

Visible–near-infrared (Vis-NIR) spectra of isolated $Gd@C_{74}(CF_3)$ (I and II) and $Gd@C_{74}(CF_3)_3$ are shown in figure 3. The quite different spectra of two mono-substituted $Gd@C_{74}(CF_3)$ species show that the two derivatives are isomers having different substituent group positions. HOMO–LUMO gaps of metallofullerenes and their derivatives can be roughly estimated from the onset in absorption spectra. $Gd@C_{74}(CF_3)$ (I), $Gd@C_{74}(CF_3)$ (II) and $Gd@C_{74}(CF_3)_3$ have the onset at 1330, 1750 and 1170 nm (figure 2), corresponding to HOMO–LUMO gap of 0.93, 0.71 and 1.06 eV, respectively. The estimated gaps of $Gd@C_{74}(CF_3)_n$ ($n = 1, 3$) are approximately close to HOMO–LUMO gaps of $Y@C_{74}(CF_3)_n$ ($n = 1, 3$), reported in our previous work [16]. In addition, the absorption spectra of $Gd@C_{74}(CF_3)$ (I, II) are also similar to those of two isomers of $La@C_{74}(C_6H_3Cl_2)$ [11]. The analogy between these Vis-NIR spectra suggests that the HOMO, LUMO and their neighbouring orbits of $M@C_{74}$ are dominated by features of the cage, irrespective of functional groups as well as encapsulated species.

Density functional calculations were performed to obtain more detailed information on the trifluoromethyl derivatives. On the basis of the structures obtained by X-ray crystal structure analysis, we carried out geometry optimizations and energy calculations on isolated pristine and functionalized $Gd@C_{74}$. Aside from small bond length changes attributable to the exchange correlation functional used, the molecular structures from X-ray analysis were confirmed as stable. Figure 4 shows optimized structures and molecular orbital energy levels. $Gd@C_{74}$ is an open-shell system in agreement with the discussion above, with HOMO energy of −4.41 eV and LUMO energy of −4.23 eV, confirming that $Gd@C_{74}$ has a very small HOMO–LUMO gap. The states lie higher in the gap than for the subsequent CF_3 functionalized species, in agreement with the experimental observation of a prevalence of positively charged species in the mass spectra. Once functionalized with CF_3 the calculated HOMO–LUMO gaps are significantly increased, with gaps for $Gd@C_{74}(CF_3)$ (I), $Gd@C_{74}(CF_3)$ (II) and $Gd@C_{74}(CF_3)_3$ of 0.92, 0.71 and 1.00 eV, respectively, consistent with those estimated from the absorption onsets. It is clear that the energy gap is enlarged considerably upon exohedral trifluoromethylation, and all three species have closed-shell configurations confirming the demonstrated stability of odd-number CF_3 additions. All three have fully unpaired Gd *f*-states, which are a pre-requisite for biomedical applications such as MRI contrast agents [3–6].

4. Discussion

The present trifluoromethylation method provides only mono- and tri-substituted derivatives [16–18]. One of the possible reasons for the selectivity is that it has an open-shell structure. Valence electrons

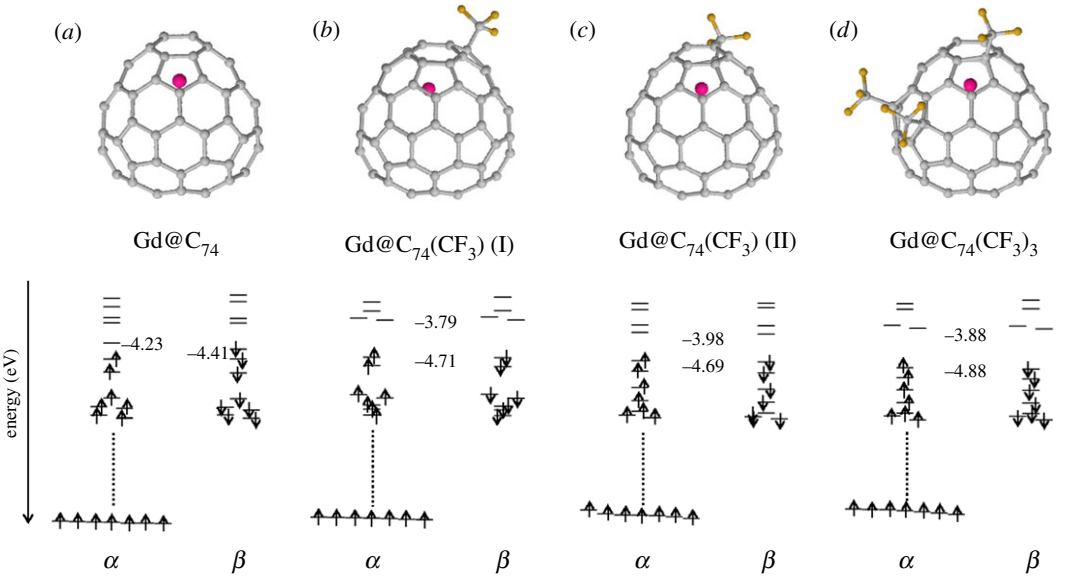

Figure 4. DFT-optimized molecular structures and corresponding calculated molecular orbital energy levels of (*a*) $Gd@C_{74}$, (*b*) $Gd@C_{74}(CF_3)$ (I), (*c*) $Gd@C_{74}(CF_3)$ (II) and (*d*) $Gd@C_{74}(CF_3)_3$.

are transferred from Gd to the cage, resulting in a charge distribution of $Gd^{3+}@C_{74}^{3-}$ [10]. Addition of odd-number CF_3 groups to the carbon cage may result in a closed-shell configuration, which is more stable than an open-shell configuration of non-substituted $Gd@C_{74}$. A similar trend has been observed in the case of previous yttrium- and lanthan-encapsulated metallofullerenes [16].

It is interesting also to examine the binding energy of CF_3 groups to the $Gd@C_{74}$ cage. Considering the reaction

$$n\tfrac{1}{2}(CF_3)_2 + Gd@C_{74} \rightarrow Gd@C_{74}(CF_3)_n,$$

we obtain a CF_3 binding energy for the two $n = 1$ isomers of 6.26 and 7.73 kcal mol^{-1}, respectively. These are close to each other, explaining the presence of both isomers (i.e. there is no single CF_3 functionalized isomer with significantly higher thermodynamic stability than any other). At the same time, the binding energy is considerably lower than for $Gd@C_{60}$ [19], which averages at 10.35 kcal mol^{-1} per CF_3 group for $Gd@C_{60}(CF_3)_5$. In the case of the $Gd@C_{74}$ $n = 3$ isomer the average binding energy per CF_3 groups drops even further to 5.78 kcal mol^{-1} (i.e. the two new CF_3 groups are each bound by only 4.81 kcal mol^{-1}), and it is reasonable to assume from this that subsequent pairwise CF_3 addition will be even less stable, presumably explaining the absence of stable $n = 5$ addition species.

5. Conclusion

In conclusion, the fullerene derivatives $Gd@C_{74}(CF_3)$ (I), $Gd@C_{74}(CF_3)$ (II) and $Gd@C_{74}(CF_3)_3$ were isolated by *in situ* trifluoromethylation followed by multi-stage HPLC purification. Their chemical structures were determined by X-ray crystal structure analysis and all of $Gd@C_{74}$ isomers have D_{3h}-symmetry cages. CF_3 groups are attached to carbon atoms on pentagons of fullerene cages. Formation of closed-shell systems and HOMO–LUMO gap widening of $Gd@C_{74}$ by the one- or three-fold addition of CF_3 group were confirmed by Vis-NIR spectra measurement and computational modelling.

Data accessibility. The crystal structures are freely available from the Cambridge Crystallographic Data Centre (CCDC) with CIF numbers 1824999 for $Gd@C_{74}(CF_3)$ (I), 1825000 for $Gd@C_{74}(CF_3)$ (II) and 1825001 for $Gd@C_{74}(CF_3)_3$. All DFT calculated structures (in xyz format) discussed in this article are provided in the electronic supplementary material associated with this article.

Authors' contributions. H.S. conceived the study, A.N., H.O., K.I., M.N. performed the synthesis, isolation and MALDI-TOF, S.A. performed the synchrotron studies, J.R. and C.E. performed the density functional calculations. All authors discussed results, helped edit the manuscript and gave final approval for publication.

Competing interests. The authors declare that they have no competing interests.

Funding. The experimental part of this work was financially supported by MEXT/JSPS KAKENHI grant numbers 16H06350, 16H02248 (H.S.) and 15K21073 to (H.O.). The theory part was financially supported by Region Pays de la Loire 'Paris Scientifiques 2017' grant number 09375 and CCIPL for computing resources. The synchrotron radiation experiments were performed at SPring-8 with the approval of the Japan Synchrotron Radiation Research Institute (JASRI) (proposal nos. 2017A1206 and 2017B1373).

References

1. Shinohara H. 2000 Endohedral metallofullerenes. *Rep. Prog. Phys.* **63**, 843–892. (doi:10.1088/0034-4885/63/6/201)
2. Shinohara H, Tagmatarchis N (eds). 2015 *Endohedral metallofullerenes: fullerenes with metal inside*. Chichester, UK: John Wiley & Sons.
3. Mikawa M, Kato H, Okumura M, Naeazaki M, Kanazawa Y, Miwa N, Shinohara H. 2001 Paramagnetic water-soluble metallofullerenes having the highest relaxivity for MRI contrast agents. *Bioconjugate Chem.* **12**, 510–514. (doi:10.1021/bc000136m)
4. Zhang J *et al.* 2010 High relaxivity trimetallic nitride (Gd_3N) metallofullerene MRI contrast agents with optimized functionality. *Bioconjugate Chem.* **21**, 610–615. (doi:10.1021/bc900375n)
5. Kato H, Kanazawa Y, Okumura M, Taninaka A, Yokawa T, Shinohara H. 2003 Lanthanoid endohedral metallofullerenols for MRI contrast agents. *J. Am. Chem. Soc.* **125**, 4391–4397. (doi:10.1021/ja027555+)
6. Gao Z, Nakanishi Y, Noda S, Omachi H, Shinohara H, Kimure H, Nakasaki Y. 2017 Development of $Gd_3N@C_{80}$ encapsulated redox nanoparticles for high-performance magnetic resonance imaging. *J. Biomater. Sci. Polym. Ed.* **28**, 1036–1050. (doi:10.1080/09205063.2017.1288774)
7. Horiguchi Y, Kudo S, Nagasaki Y. 2011 $Gd@C_{82}$ metallofullerenes for neutron capture therapy—fullerene solubilization by poly(ethylene glycol)-block-poly(2-(N, N-diethylamino)ethyl methacrylate) and resultant efficacy *in vitro*. *Sci. Technol. Adv. Mater.* **12**, 44607. (doi:10.1088/1468-6996/12/4/044607)
8. Liang X-J *et al.* 2010 Metallofullerene nanoparticles circumvent tumor resistance to cisplatin by reactivating endocytosis. *Proc. Natl Acad. Sci. USA* **107**, 7449–7454. (doi:10.1073/pnas.0909707107)
9. Diener MD, Alford JM. 1998 Isolation and properties of small-bandgap fullerenes. *Nature* **393**, 668–671. (doi:10.1038/31435)
10. Wan TSM, Zhang HW, Nakane T, Xu Z, Inakuma M, Shinohara H, Kobayashi K, Nagase S. 1998 Production, isolation, and electronic properties of missing fullerenes: $Ca@C_{72}$ and $Ca@C_{74}$. *J. Am. Chem. Soc.* **120**, 6806–6807. (doi:10.1021/ja972478h)
11. Nikawa H *et al.* 2005 Missing metallofullerene $La@C_{74}$. *J. Am. Chem. Soc.* **127**, 9684–9685. (doi:10.1021/ja0524806)
12. Wakahara T *et al.* 2006 $La@C_{72}$ having a non-IPR carbon cage. *J. Am. Chem. Soc.* **128**, 14 228–14 229. (doi:10.1021/ja064751y)
13. Xu J, Tsuchiya T, Hao C, Shi Z, Wakahara T, Mi W, Gu Z, Akasaka T. 2006 Structure determination of a missing-caged metallofullerene: $Yb@C_{74}$ (II) and the dynamic motion of the encaged ytterbium ion. *Chem. Phys. Lett.* **419**, 44–47. (doi:10.1016/j.cplett.2005.11.045)
14. Lu X, Nikawa H, Kikuchi T, Mizorogi N, Slanina Z, Tsuchiya T, Nagase S, Akasaka T. 2011 Radical derivatives of insoluble $La@C_{74}$: X-ray structures, metal positions, and isomerization. *Angew. Chem. Int Ed.* **50**, 6356–6359. (doi:10.1002/anie.201100961)
15. Maeda Y *et al.* 2016 Effective derivatization and extraction of insoluble missing lanthanum metallofullerenes $La@C_{2n}$($n = 36–38$) with iodobenzene. *Carbon* **98**, 67–73. (doi:10.1016/j.carbon.2015.10.088)
16. Wang Z, Nakanishi Y, Noda S, Niwa H, Zhang JY, Kitaura R, Shinohara H. 2013 Missing small-bandgap metallofullerenes: their isolation and electronic properties. *Angew. Chem. Int. Ed.* **52**, 11770–11774. (doi:10.1002/anie.201305573)
17. Wang Z, Aoyagi S, Omachi H, Kitaura R, Shinohara H. 2015 Isolation and structure determination of a missing endohedral fullerene $La@C_{70}$ through *in situ* trifluoromethylation. *Angew. Chem. Int. Ed.* **55**, 199–202. (doi:10.1002/anie.201508082)
18. Xu D, Wang Z, Shinohara H. 2017 Capturing the unconventional metallofullerene $M@C_{66}$ by trifluoromethylation: a theoretical study. *ChemPhysChem* **18**, 3007–3011. (doi:10.1002/cphc.201700830)
19. Nakagawa A *et al.* 2018 Crystalline C_{60} fulleride with metal inside. *Nature Commun.* **9**, 3073. (doi:10.1038/s41467-018-05496-8)
20. Boltalina OV, Popov AA, Kuvychko IV, Shustova NB, Strauss SH. 2015 Perfluoroalkylfullerenes. *Chem. Rev.* **115**, 1051–1105. (doi:10.1021/cr5002595)
21. Kareev IE, Kuvychko IV, Lebedkin SF, Miller SM, Anderson OP, Seppelt K, Strauss SH, Boltalina OV. 2005 Structure, and ^{19}F NMR spectra of 1,3,7,10,14,17,23,28,31,40-$C_{60}(CF_3)_{10}$. *J. Am. Chem. Soc.* **127**, 8362–8375. (doi:10.1021/ja050305j)
22. Kareev IE, Lebedkin SF, Bubnov VP, Yagubskii EB, Ioffe IN, Khavrel PA, Kuvychko IV, Strauss SH, Boltalina OV. 2005 Trifluoromethylated endohedral metallofullerenes: synthesis and characterization of $Y@C_{82}(CF_3)_5$. *Angew. Chem. Int. Ed.* **117**, 1880–1883. (doi:10.1002/ange.200461497)
23. Popov AA, Kareev IE, Shustova NB, Stukalin EB, Lebedkin SF, Seppelt K, Strauss SH, Boltalina OV, Dunsch L. 2007 Electrochemical, spectroscopic, and DFT study of $C_{60}(CF_3)n$ frontier orbitals ($n = 2–18$): the link between double bonds in pentagons and reduction potentials. *J. Am. Chem. Soc.* **129**, 11 551–11 568. (doi:10.1021/ja073181e)
24. Akiyama K, Hamano T, Nakanishi Y, Takeuchi E, Noda S, Wang ZY, Kubuki S, Shinohara H. 2012 Non-HPLC rapid separation of metallofullerenes and empty cages with $TiCl_4$ Lewis acid. *J. Am. Chem. Soc.* **134**, 9762–9767. (doi:10.1021/ja3030627)
25. Wang Z, Nakanishi Y, Noda S, Akiyama K, Shinohara H. 2012 The origin and mechanism of non-HPLC purification of metallofullerenes with $TiCl_4$. *J. Phys. Chem. C* **116**, 25 563–25 567. (doi:10.1021/jp307729j)
26. Wang Z, Omachi H, Shinohara H. 2017 Non-chromatographic purification of endohedral metallofullerenes. *Molecules* **22**, 718. (doi:10.3390/molecules22050718)
27. Sugimoto K, Ohsumi H, Aoyagi S, Nishibori E, Moriyoshi C, Kuroiwa Y, Sawa H, Takata M. 2010 Extremely high resolution single crystal diffractometry for orbital resolution using high energy synchrotron radiation at SPring-8. *AIP Conf. Proc.* **1234**, 887–890. (doi:10.1063/1.3463359)
28. Burla MC, Caliandro R, Carrozzini B, Cascarano GL, Cuocci C, Giacovazzo C, Mallamo M, Mazzone A, Polidori G. 2015 Crystal structure determination and refinement via SIR2014. *J. Appl. Cryst.* **48**, 306–309. (doi:10.1107/s1600576715001132)
29. Sheldrick GM. 2015 Crystal structure refinement with SHELXL. *Acta Cryst.* **C71**, 3–8. (doi:10.1107/s2053229614024218)
30. Schomaker V, Trueblood KN. 1968 On the rigid-body motion of molecules in crystals. *Acta Cryst.* **B24**, 63–76. (doi:10.1107/s0567740868001718)
31. Sado Y, Aoyagi S, Kitaura R, Miyata Y, Nishibori E, Sawa H, Sugimoto K, Shinohara H. 2013 Structure of $Tm@C_{82}$(I) metallofullerene by single-crystal X-ray diffraction using the 1:2 co-crystal with octaethylporphyrin nickel (Ni(OEP)). *J. Phys. Chem. C* **117**, 6437–6442. (doi:10.1021/jp311948c)
32. Rayson MJ, Briddon PR. 2008 Rapid iterative method for electronic-structure eigenproblems using localised basis functions. *Comput. Phys. Commun.* **178**, 128–134. (doi:10.1016/j.cpc.2007.08.007)
33. Rayson MJ, Briddon PR. 2009 Highly efficient method for Kohn-Sham density functional calculations of 500–10 000 atom systems. *Phys. Rev. B* **80**, 205104. (doi:10.1103/physrevb.80.205104)
34. Briddon PR, Rayson MJ. 2011 Accurate Kohn-Sham DFT with the speed of tight binding:

current techniques and future directions in materials modelling. *Phys. Status Solidi B* **248**, 1309–1318. (doi:10.1002/pssb.201046147)

35. Hartwigsen C, Goedecker S, Hutter J. 1998 Relativistic separable dual-space Gaussian pseudopotentials from H to Rn. *Phys. Rev. B* **58**, 3641–3662. (doi:10.1103/physrevb.58.3641)
36. Goss JP, Shaw MJ, Briddon PR. 2007 Marker-method calculations for electrical levels using Gaussian-orbital basis sets. *Topics Appl. Phys.* **104**, 69–94. (doi:10.1007/11690320_4)
37. Ewels C, Rio J, Niwa H, Omachi H, Shinohara H, Rayson M, Briddon P. 2018 Determining addition pathways and stable isomers for CF_3 functionalization of endohedral Gd@C_{60}. *R. Soc. open sci.* **5**, 180588. (doi:10.1098/rsos.180588)
38. Suzuki M, Lu X, Sato S, Nikawa H, Mizorogi N, Slanina Z, Tsuchiya T, Nagase S, Akasaka T. 2012 Where does the metal cation stay in Gd@C_{2v}(9)-C_{82}? A single-crystal X-ray diffraction study. *Inorg. Chem.* **51**, 5270–5273. (doi:10.1021/ic300186y)